ELSEVIER

Journal of Alloys and Compounds 330–332 (2002) 183–186

Journal of ALLOYS AND COMPOUNDS

www.elsevier.com/locate/jallcom

Site determination of positive muons in Pr single crystal

F.N. Gygax*, D. Andreica, M. Pinkpank, A. Schenck

Institute for Particle Physics of ETH Zürich, CH-5232 Villigen PSI, Switzerland

Abstract

Pr, with a dhcp crystal structure, possesses a strongly anisotropic bulk magnetic susceptibility χ. The temperature dependencies of $\chi_{\parallel}$ (applied magnetic field $\boldsymbol{H}_{ext}$ parallel to c axis) and $\chi_{\perp}$ (field perpendicular to c axis) are quite different; they can be described by two distinct Curie–Weiss forms at high temperature. Transverse-field (TF) μSR measurements have been performed in a single-crystal Pr sample. In the studied temperature range ($1.8 \leq T \leq 300$ K), depending on the crystal orientation in $\boldsymbol{H}_{ext}$, a single frequency precession signal is obtained, from which the two principal Knight-shift (K_{μ}) components can be determined. For $\boldsymbol{H}_{ext} \perp \boldsymbol{c}$ a linear scaling between K_{μ} and χ is found for the entire T range. For $\boldsymbol{H}_{ext} \| \mathbf{c}$ a linear scaling is only observed above 50 K. From these K_{μ} vs. χ relations the axial dipolar-coupling tensor A^{D} is deduced. Candidates for hosting the μ^{+} in Pr are e sites and f sites (Wyckoff notation) of the $P6_3/mmc$ crystal structure. For both sites we have calculated the dipolar-coupling tensor, and found an agreement with the measurements only for the f sites (octahedral interstices). Thus it appears that the muon resides at f sites.

Keywords: Pr; Muon Knight shift; Muon site

1. Introduction

We have implanted positive muons in a Pr single crystal and performed μSR spectroscopy. In the present report we discuss the μ^{+} Knight shift obtained from transverse-field (TF) measurements.

Pr, with a dhcp crystal structure, possesses a strongly anisotropic bulk magnetic susceptibility χ. The temperature dependencies of $\chi_{\parallel}$ (applied magnetic field $\boldsymbol{H}_{ext}$ parallel to c axis) and $\chi_{\perp}$ (field perpendicular to c axis) are quite different; they have been measured for material cut from our specimen, Fig. 1[1]. At the higher temperatures the two χ components can be described by a Curie–Weiss law, i.e. above 30 K for $\chi_{\perp}$, with the paramagnetic Curie temperature $\Theta_{\perp} = 11.8$ K, and only above 50 K for $\chi_{\parallel}$, with a negative $\Theta_{\parallel}$ of -28.4 K.

We used a single-crystal Pr sample of nearly cylindrical shape, diameter ~9 mm and length 30 mm, with its [110] direction parallel to the cylinder axis.

2. Muon Knight shift

TF measurements have been performed in two experimental set-ups: 'Strobo' and 'GPD', Fig. 2. In Strobo the crystal orientation can be modified by rotating the

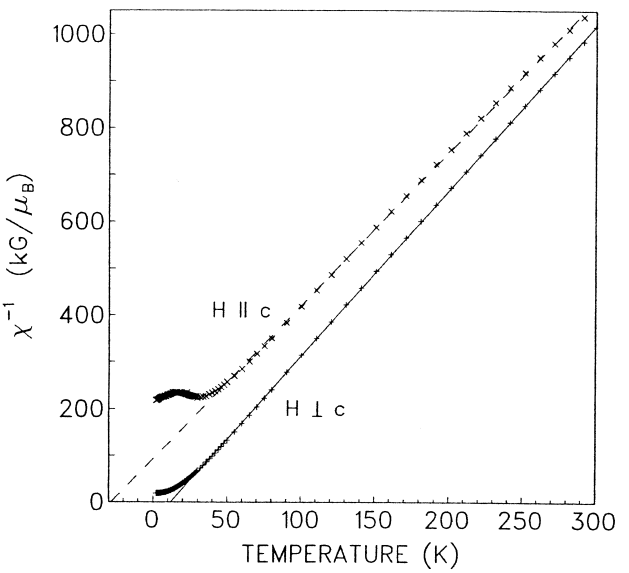

Fig. 1. Temperature dependence of the inverse bulk magnetic susceptibility measured in the Pr single crystal; × for for $\boldsymbol{H}_{ext} \| \boldsymbol{c}$, + for $\boldsymbol{H}_{ext} \perp \boldsymbol{c}$. The straight lines are Curie–Weiss relations.

*Corresponding author. Tel.: +41-56-310-3225; fax: +41-56-310-4362.

E-mail address: fredy.gygax@psi.ch (F.N. Gygax).

[1]We are grateful to G.J. Niewenhuys (Leiden) for help and equipment which allowed to determine the magnetic susceptibility of the sample.

0925-8388/02/$ – see front matter
PII: S0925-8388(01)01629-2

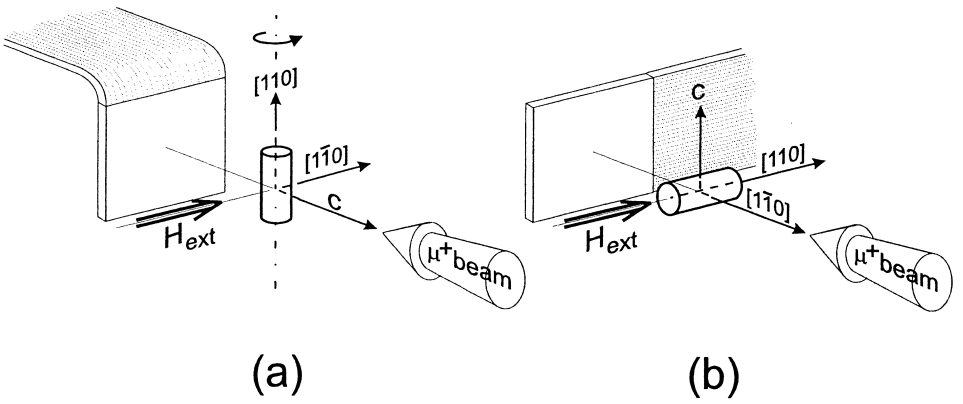

Fig. 2. Diagram of the geometries used for the Knight-shift measurements, indicating also the position of the forward-decay detector. (a) Strobo set-up, with possibility to rotate the sample to change the orientation angle Θ of the crystal c axis in the field, $0 \leq \Theta \leq 180°$. (b) GPD set-up, with fixed crystal orientation, $\Theta = 90°$.

sample around its [110] direction, perpendicular to $\boldsymbol{H}_{ext}$. This allows a full scan of the angle Θ between crystal c axis and $\boldsymbol{H}_{ext}$, thus including $\boldsymbol{H}_{ext} \| \boldsymbol{c}$ as well as $\boldsymbol{H}_{ext} \perp \boldsymbol{c}$, i.e. $\boldsymbol{H}_{ext}$ in the crystal basal plane. For the full studied temperature range ($1.8 \leq T \leq 300$ K) and for all crystal orientations a single frequency μSR signal, stemming from the sample, is observed – in addition to a set-up dependent (but basically constant) background signal, stemming from the cryogenic sample environment.

The sample signal was well fitted, either with an exponential relaxation function, or even better, specially at lower temperatures, with a Gaussian relaxation function (with identical result in terms of the determined frequency). These signals have been measured in three geometries: the cylinder axis of the sample transverse to the field as in Fig. 2(a), (i) with the applied field $\boldsymbol{H}_{ext} \perp \boldsymbol{c}$, and (ii) with $\boldsymbol{H}_{ext} \| \boldsymbol{c}$, and (iii) the cylinder axis longitudinal in the field, with $\boldsymbol{H}_{ext} \perp \boldsymbol{c}$, as in Fig. 2(b).

To determine the Knight shift K_μ starting from the raw μSR frequency shifts obtained in the TF measurements, a demagnetization-field correction, together with the Lorentz-field correction, have to be applied. From the two measurements with $\boldsymbol{H}_{ext} \perp \boldsymbol{c}$, first with the sample cylinder transverse to the field, then with the cylinder longitudinal, along the field, the difference of the effective demagnetization factors $N_T - N_L$ (T for transverse and L for longitudinal) is obtained. With this value and the demagnetization factors for cylindrical samples calculated by Akishin and Gaganov [1] the effective sample parameters, hence

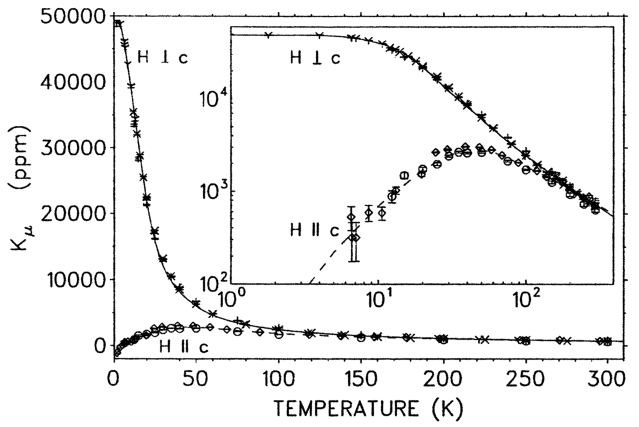

Fig. 3. Temperature dependence of the two μ^+ Knight-shift components, five measurement series. Circles and diamonds for $\boldsymbol{H}_{ext} \| \boldsymbol{c}$, stars and + marks for $\boldsymbol{H}_{ext} \perp \boldsymbol{c}$. For the insert the axes are logarithmic.

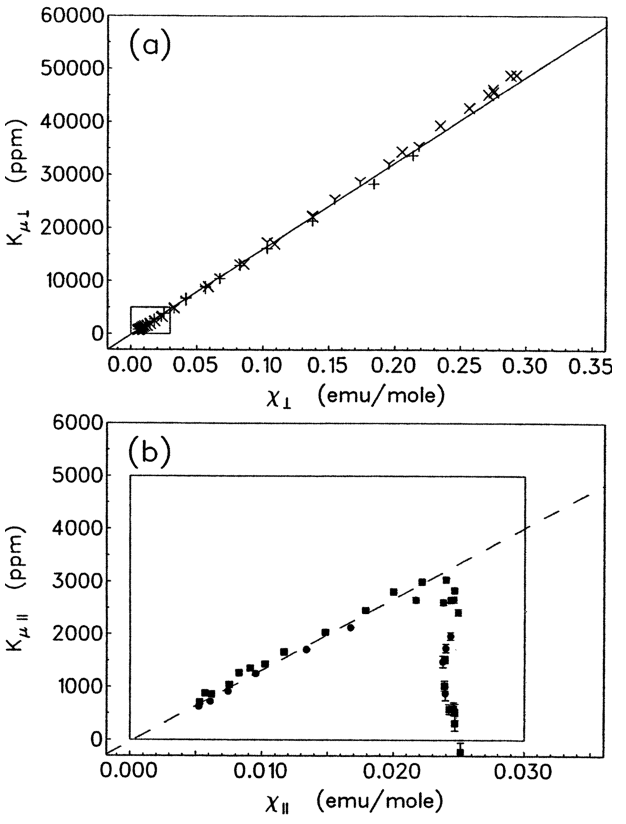

Fig. 4. μ^+ Knight shift represented versus bulk susceptibility (Clogston–Jaccarino plots); (a) magnetic field perpendicular to the crystal c axis, (b) magnetic field parallel to the c axis. Notice the scale difference: the inner rectangle of both graphs frames the same $\chi \times K_\mu$ domain.

the effective N_T and N_L demagnetization factors, are determined. After application of the combined demagnetization-field and Lorentz-field correction, five $K_\mu(T)$-measurement series are obtained: at 0.33 T, 0.40 T and 0.63 T with $\boldsymbol{H}_{ext}\perp\boldsymbol{c}$, and at 0.33 T and 0.63 T with $\boldsymbol{H}_{ext}\|\boldsymbol{c}$. The five dependencies are shown in Fig. 3; the reproducibility of $K_{\mu\perp}(T)$ and $K_{\mu\|}(T)$, obtained under quite different experimental conditions, is very good. In addition we have measured $K_\mu(T)$ at a much lower field, 20 mT. Also these values do not present any deviation from the results obtained between 0.33 and 0.63 T. As usual, the Knight-shift measurement at low field are less precise, thus the 20 mT data do not contribute to the ultimate average.

Fig. 4 shows the two Knight-shift components represented versus the respective bulk susceptibility components, with the temperature as implicit parameter. For $\boldsymbol{H}_{ext}\perp\boldsymbol{c}$ a linear scaling is seen over the entire studied temperature range $T \geq 1.8$ K, with a slope $\Delta K_\mu/\Delta\chi = 0.158(2)$ mole emu^{-1}. For $\boldsymbol{H}_{ext}\|\boldsymbol{c}$ a linear scaling is only observed above 50 K, with $\Delta K_\mu/\Delta\chi = 0.135(4)$ mole emu^{-1}. Interestingly, the pronounced departure of $K_{\mu\|}(\chi_\|)$ from the linear behavior observed at high temperature happens for $T \leq 50$ K, where also $\chi_\|$ deviates from a Curie–Weiss law.

3. Determination of μ^+ site

In the elementary cell of the dhcp $P6_3/mmc$ structure of Pr ($a \approx 3.67$ Å, $c \approx 11.83$ Å), two of the four atoms occupy the a position (Wyckoff notation), (0,0,0) and (0,0,$\frac{1}{2}$), and the two other the c positions, ($\frac{1}{3},\frac{2}{3},\frac{1}{4}$) and ($\frac{2}{3},\frac{1}{3},\frac{3}{4}$) – Fig. 5. Candidates for hosting the μ^+ are the 4e positions, e.g. (0,0,z), and the 4f positions, e.g. ($\frac{1}{3},\frac{2}{3},z$). The e and f sites have axial symmetry.

In that case the Knight shift will take the form [2]:

$$K_{\mu\|}(T) = (A_c + A^D_{cc})\chi_\|(T) \quad (1)$$

and

$$K_{\mu\perp}(T) = (A_c + A^D_{aa})\chi_\perp(T) = (A_c - \frac{1}{2}A^D_{cc})\chi_\perp(T). \quad (2)$$

A_c is the contact hyperfine-field coupling constant, A^D_{aa} and A^D_{cc} the components of the dipolar-coupling tensor

$$\overleftrightarrow{A}^D = \begin{pmatrix} A^D_{aa} & 0 & 0 \\ 0 & A^D_{aa} & 0 \\ 0 & 0 & A^D_{cc} \end{pmatrix}.$$

$\chi_\|$ and $\chi_\perp$ are the components of the axially symmetric susceptibility tensor $\overleftrightarrow{\chi}^{at}$, here susceptibility per atom, assumed to be given by the bulk susceptibility: $\overleftrightarrow{\chi}^{at} = \overleftrightarrow{\chi}^{mole}/N_A$, where N_A is Avogadro's number.

The determined scaling coefficients $\Delta K_\mu/\Delta\chi$ quoted above are the non-zero components of the local field tensor at the μ^+ site (for this purpose the coefficients have to be converted from mole emu^{-1} into kG/μ_B): $\overleftrightarrow{A}^L = \overleftrightarrow{A}^D + A_c \overleftrightarrow{E}$, where $\overleftrightarrow{E}$ is the unit tensor. Thus one has $A^L_{aa} = A^L_{bb} = 0.882(112)$ kG/μ_B, and $A^L_{cc} = 0.754(234)$ kG/μ_B. Considering that $\mathrm{Tr}(\overleftrightarrow{A}^D) = 0$, one obtains in our case

$$\overleftrightarrow{A}^D = \begin{pmatrix} 0.043(12) & 0 & 0 \\ 0 & 0.043(12) & 0 \\ 0 & 0 & -0.086(24) \end{pmatrix} \mathrm{kG}/\mu_B.$$

For comparison we have calculated the dipolar-coupling tensor for the e and f sites. Fig. 6 shows the A^D_{aa} components as functions of the z positions for the two site types, together with the A^D_{aa} values determined experimentally. The possible μ^+ sites are tetrahedral (T) interstices for the e positions and octahedral (O) interstices for the f positions. Tetrahedron and octahedron are nearly regular, the edges differ by less than 1%. For the e site at the center of the tetrahedron, with, e.g. $z = 0.1896$ (distance to the nearest Pr atom: 2.24 Å), one has $\overleftrightarrow{A}^D = 0$. The measured

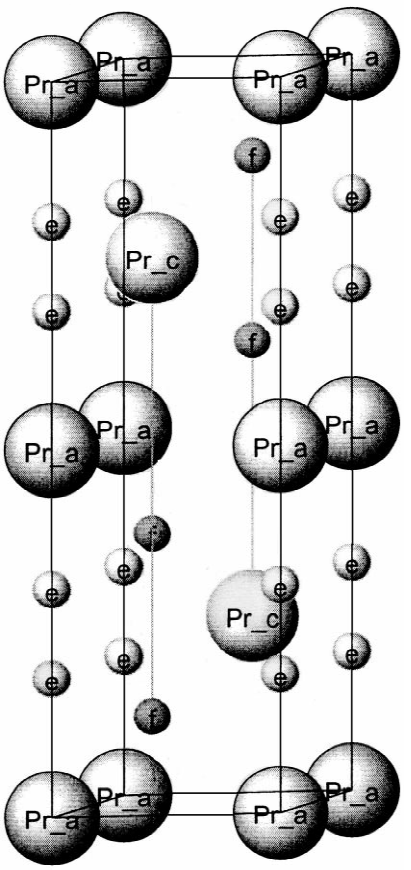

Fig. 5. Unit cell of the dhcp Pr crystal, containing two atoms in a sites, with $z = 0$ and $\frac{1}{2}$, and two atoms at c sites, with $z = \frac{1}{4}$ and $\frac{3}{4}$. Candidates for μ^+ locations are the tetrahedral 4e sites, e.g. (0,0,z) (small light spheres), and the octahedral 4f sites, e.g. ($\frac{1}{3},\frac{2}{3},z$) (small grey spheres).

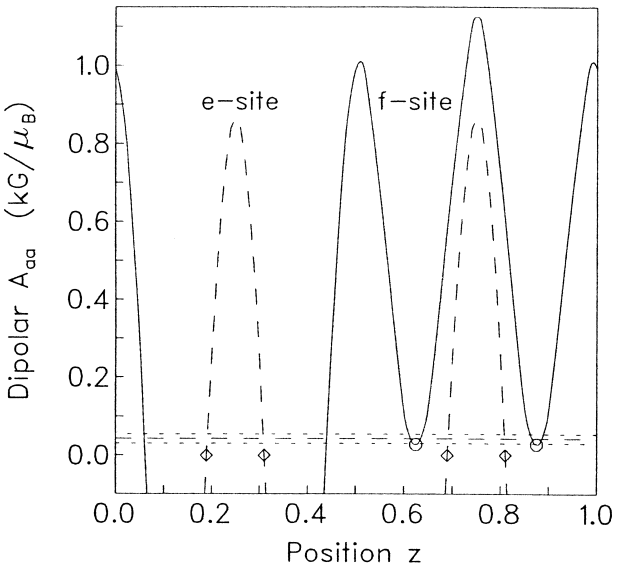

Fig. 6. Pr single crystal, dhcp structure. Calculated dipolar-coupling tensor components A^{D}_{aa} as functions of the z positions of the f site, $(\frac{1}{3},\frac{2}{3},z)$, solid line, and the e site, $(0,0,z)$, dashed line. f sites at the center of octahedral interstices are marked by ○, e sites at the center of tetrahedral interstices by ◊. The band between the dotted horizontal lines indicates the measured A^{D}_{aa} value with its error.

A^{D}_{aa} value is close, but clearly not compatible with zero. The μ^+ would have to be $\sim 0.9\%$ farther away from the nearest Pr atom along the z-axis to experience an A^{D}_{aa} value as measured. For the f sites at the center of the octahedron, with, e.g. $z = 0.625$ (distance to the nearest Pr atoms: 2.59 Å), $A^{D}_{aa} = 0.03$ is calculated, in excellent agreement with the measured value. In addition the z dependence of the A^{D}_{aa} component has a minimum at that position, contrary to the situation at the T-interstitial e site, where the variation of A^{D}_{aa} along z is important. This gives a guarantee that for muons at f sites no drastic broadening (e.g. due to crystal imperfections) will prevent or complicate the determination of the dipolar-coupling tensor – and in fact the $\overleftrightarrow{A}^{D}$ components have been determined readily from the measurements.

For the calculation of $\overleftrightarrow{A}^{D}$ we assumed no crystal relaxation around the μ^+. A lattice distortion (usually a fairly isotropic displacement of the nearest atoms surrounding the muon, changing the distance muon–atom by a few percents) results in a small reduction of the average local magnetic fields at the μ^+ site and/or of the related dipolar-coupling tensor components. This would not imply a fundamentally different situation from the undisturbed case when comparing calculations to measurements.

Not much is known about H in Pr in the solid-solution α phase, α-PrH_x [3]. Particularly, we could not find any mention of the H (or D) location. For most other rare-earth elements, which to the contrary of Pr crystallize in the simple hcp structure, H is located at T sites [3]. The same is valid for the μ^+ – in the case of Sc, moreover, a fast local μ^+ hopping between adjacent T sites is observed [4].

From the present observations it appears that the muon resides at f sites in Pr.

References

[1] P.G. Akishin, I.A. Gaganov, J. Magn. Magn. Mater. 110 (1992) 175.
[2] A. Schenck, in: S.L. Lee, S.H. Kilcoyne, R. Cywinsky (Eds.), Muon Science, SUSSP Publications and Institute of Physics Publishing, Bristol, 1999, p. 39.
[3] See, e.g., P. Vajda, Hydrogen in Rare-Earth Metals, Including RH_{2+x}, Handbook on the Physics and Chemistry of Rare Earths, Vol. 20, K.A. Gschneidner, Jr., L. Eyring (Eds.), Elsevier, New York, 1995, p. 207, and references therein.
[4] F.N. Gygax, G. Solt, A. Amato, I.S. Anderson, M. Pinkpank, A. Schenck, T.J. Udovic, Phys. Rev. B 61 (2000) 168.